ROG.e 2024

ISSN 2525-7579

Conference Proceedings homepage: https://biblioteca.ibp.org.br/riooilegas

Technical Paper

Comparison of hot-wire and cold-wire GTAW with dynamic wire feeding of Inconel 625 deposits for cladding applications

Ivan Olszanski Pigozzo [1]
Régis Henrique Gonçalves e Silva [2]
Alberto Bonamigo Viviani [3]
Guilherme Meurer [4].

1. UNIVERSIDADE FEDERAL DE SANTA CATARINA, ENG. MACÂNICA, . FLORIANÓPOLIS - SC - BRASIL, IVANPIGOZZO@GMAIL.COM 2. UNIVERSIDADE FEDERAL DE SANTA CATARINA, ENG. MACÂNICA, . FLORIANÓPOLIS - SC - BRASIL, REGIS.SILVA@UFSC.BR 3. UNIVERSIDADE FEDERAL DE SANTA CATARINA, ENG. MACÂNICA, . FLORIANÓPOLIS - SC - BRASIL, ALBERTO.BONAMIGO@POSGRAD.UFSC.BR 4. UNIVERSIDADE FEDERAL DE SANTA CATARINA, ENG. MACÂNICA, . FLORIANÓPOLIS - SC - BRASIL, GUINOGUEIRA2013@GMAIL.COM

Abstract

Gas tungsten arc welding process are widely used for cladding and surface repairing. In oil & Gas industry, Ni-Cr alloys stand out for severe corrosion associated to high temperature conditions. In this study, cold-wire and hot-wire GTAW tests conciliated with dynamic wire feeding were carried out to evaluated Inconel 625 deposits. Single beads and overlay samples were deposited over ASTM A36 low carbon steel plates with 9,35 mm thick. The experiments were conducted with a welding current of 170 A and, for hot-wire tests, 70 A. The wire feed speed was set in 25 mm/s and, for sample with dynamic wire feeding, the wire oscillation frequency was 18 Hz. Arc length, travel speed was the same for all conditions. The results shown that samples carried out with dynamic wire feeding for both conditions (cold-wire and hot-wire) had lower penetration and greater reinforcement, compared to samples with conventional wire feeding. Furthermore, the weld bead width reduced when dynamic wire feeding was used. Regarding the dilution, samples carried out with dynamic wire feeding shown lower dilution for cold-wire and hot-wire tests, even though, the hot-wire samples shown greater dilution than cold-sire samples. Spectroscopy was also done to evaluate the percentage of Fe in the overlay samples surface. The cold-wire samples shown less Fe in the surface than hot-wire samples, but tests carried out with dynamic wire feeding result in less Fe on surface for both conditions.

Keywords: hot-wire; inconel 625; dynamic wire feeding; GTAW; cladding.

Received: November 01, 2023 | **Accepted:** | **Available online:**
Article nº:
Cite as: Proceedings of the ROG.e, Rio de Janeiro, RJ, Brazil, 2024.
DOI: https://doi.org/10.48072/2525-7579.rog.2024.

1. Introduction

Surface coating procedures consists of deposits of a specific alloys over a substrate, to enhance the performance and mechanical properties of the parts in service. The surface modification of components is a critical field of research in the oil and gas industry (Abioye, Folkes, Clare and McCartney, 2015). Over the many methods for overlaying, welding processes stand out due its strong metallurgical bonding with base material and reduced equipment costs (Rozmus-Górnikowska, Blicharski and Kusinski, 2013). For such applications, the GTAW (Gas Tungsten Arc Welding) process is recognized by its good arc controllability and robustness, promoting high quality coatings (Saha and Das, 2016).

In Oil & Gas industry, parts are commonly subjected to aggressive environments of corrosion and heat. In this scenario, Ni-based alloys, particularly the commercial alloy known as Inconel 625 (ER NiCrMo-3), excel in high-temperature corrosion resistance. Still, one of the main requirements of the resultant overlay is low dilution and reduced thickness (Silwal, Walker and West, 2019).

Besides the conventional methods for wire feeding in GTAW process, the hot-wire (preheated wire) configuration allows a lower heat input and higher deposition rate when compared to cold-wire (Siwal and Santangelo, 2018). Moreover, new wire feeding techniques, such as the dynamic wire feeding (wire longitudinal oscillation), have been investigated by many research groups. Riffel et al. (2020) obtained lower dilution for single beads of Inconel 625 deposited t with dynamic wire feeding.

The present work aims to compare the GATW process with cold-wire and hot-wire configuration, and the dynamic wire feeding, to evaluate Inconel 625 deposits for cladding applications.

2. Materials and Methods

Single beads and overlay deposits of Inconel 625 were carried out over ASTM A36 low carbon steel plates with 9.35 mm thickness. The filler wire diameter used was 1.0 mm. TABLE 1 and Table **2** show the chemical composition of base and filler metal respectively.

For shielding gas, pure argon (99.99 % level of purity) was used, and the electrode was an WGLa-15 with 3.2 mm diameter and 45° of sharpening angle. In the present work, the wire was inserted in the arc/molten pool through its front region. The wire feeding angle was fixed in 50° relative to the electrode axis, and the distance electrode-to-wire (DEW) was 4 mm.

Table 1 - Inconel 625 chemical composition

AWS ER NiCrMo-3 wire composition													
Elmt	C	Mn	Fe	P	S	Si	Cu	Ni	Al	Ti	Cr	Nb	Mo
%Wt	≤ 0.10	≤ 0.50	≤ 5.00	≤ 0.02	≤ 0.015	≤ 0.50	≤ 0.50	≥ 58.0	≤ 0.40	≤ 0.40	20.0 – 23.0	3.15 – 4.15	8.0 – 10.0

Table 2 – ASTM A36 chemical composition.

ASTM A36 plate composition									
Element	C	Mn	Si	S	P	Cu	Cr	Ni	Mo
Wt-%	0.14	0.51	0.17	0.014	0.016	0.10	0.11	0.05	0.012

The welding procedures were executed in flat position where the torch displacement was executed by a TIPTIG Tractor and power source was a TIPTIG 500i AC HW/CW. Th TIPTIG setup also provides the wire oscillation with fixed frequency of 18 Hz. During the experiments, the substrate plate remained stationary while the torch was moved across the workbench. The welding current (I), arc voltage (Uarc), electrode-to-wire voltage (Uew) and hot-wire currents (I_{HW}) were acquired by means of a data acquisition system at a sampling rate of 2 kHz. The acquired data was later processed and analyzed with the MATLAB software.

The experimental array concerned four experiments combing cold-wire and hot-wire with wire oscillation (dynamic wire feeding) and conventional wire feeding. Later, overlay samples were conducted with torch weaving. The experimental array and welding parameter used are shown in

Table **3** and

Table 4.

For macrographic analysis, the samples were cut, grinded (80 to 1200 grit sizes), polished with alumina solution (AL2O3) and etched with Nital 2%. To evaluate the Fe content in the weld bead surfaces, Optical Emission Spectrometry (OES) was performed. The weld bead dilution was measured by two methods: geometrical and chemical analysis. The geometric analysis is illustrated by Figure 1 and considers the ratio between the diluted area and total molten area. The chemical analysis is conducted through Equation 1

$$D = \frac{\%Fe\ (measured) - \%Fe\ (wire\ composition)}{\%\ Fe\ (base\ metal\ composition)} \quad (1)$$

where %Fe in the wire composition is 5 % and the % Fe of base metal is 99 %.

Table 3 – Experimental array.

Experiments description	
CW-CWF	Cold-Wire – Conventional Wire Feeding
CW-DWF	Cold-Wire – Dynamic Wire Feeding
HW-CWF	Hot-Wire – Conventional Wire Feeding
HW-DWF	Hot-Wire – Dynamic Wire Feeding

Table 4 – Welding parameters.

Experiments	CW-CWF	CW-DWF	HW-CWF	HW-DWF
Hot Wire Current [A]	-	-	70	70
Welding Current [A]	170			
Wire oscillation frequency [Hz]	18			
Wire feed speed [mm/s]	25			
Travel speed [mm/s]	2.2			
Arc Length [mm]	4			
Wire insertion angle	50			
Electrode to wire distance [mm]	4			
Gas flow rate [l/min]	15			
Overlay samples weaving Parameters				
Weaving amplitude [mm]	10			
Weaving frequency [Hz]	1			

Figure 1 – Macrographic cross section. Geometric dilution.

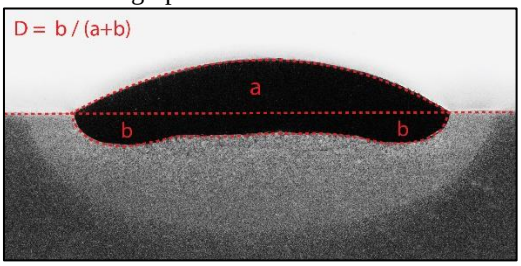

Source: developed by the authors.

3. Results and Discussions

Figure 2 represents the electrical signals (Arc voltage, Electrode-to-wire voltage, Arc current and hot-wire current) oscillograms for each conditions tested. For the samples carried out with conventional wire feeding (CW-CWF and HW-CWF), the signals are kept constant, with slight variations on the voltage values due to the molten pool oscillation or eventual droplet detachments. As it can be seen in the oscillogram of the HW-DWF sample, the sudden decrease of the Electro-to-wire voltage (U_{WE}) represents the rupture of the metallic bridge in between the wire and molten pool. During the detachment period, the hot-wire current (I_{HW}) is “zero” and the arc voltage (U_{ARC}) has a small decrement.

Figure 2 – Arc voltage (Uarc), electrode-to-wire voltage (Uwe), arc current (Iarc) and hot-wire current (Ihw) oscillograms.

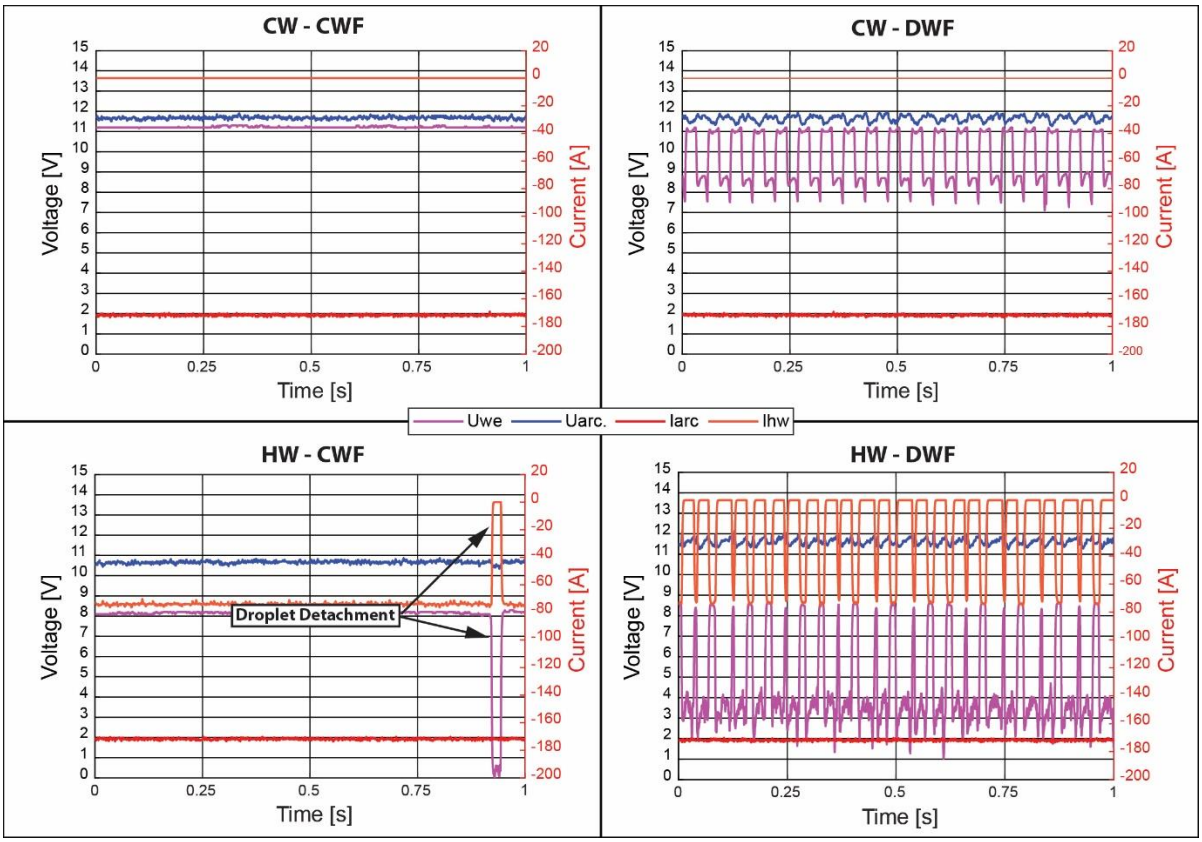

Source: developed by the authors

For dynamic wire feeding samples, the Uwe oscillates with wire movement, signifying metal bridge establishment (high voltage) and rupture (low voltage). The arc voltage also oscillates due to the arc anchoring position as described by Silva, et al. (2019) For the HW-DWF the hot wire current also oscillates accordingly to the U_{WE} signal. During the detachments period, the I_{HW} remains null until the next metal bridge is established.

Still on Figure 2 – Arc voltage (Uarc), electrode-to-wire voltage (Uwe), arc current (Iarc) and hot-wire current (Ihw) oscillograms., comparing experiments with dynamic wire feeding, cold-wire samples show a stable, uniform metal transfer. Uwe signals depict well-defined, cyclical detachments, with similar periods (approx. 29 ms). On the other hand, hot-wire samples exhibit shorter detachment periods, due to faster wire melting, leading to earlier metal bridge rupture. Additionally, rapid detachments can be observed in the HW-DWF oscillogram. These events represent the transfer of a droplet retained in the wire's tip from the previous cycle, which is rapidly transferred to the molten pool by surface

tension. The elapsed time for these detachments is approximately 6 ms, contrasting with the 15 ms duration of other detachments.

The electrical signals acquired (Table 5) shows consistent arc power (1986 W) across experiments, despite slight voltage variations due to dynamic wire feeding, leading to higher standard deviations for cold-wire and hot-wire conditions while maintaining average arc power. In the HW-CWF sample, the lower arc voltage (11.1 V) resulted in lower arc power (1922 W), even though the difference is less than 5%, compared to the HW-DWF sample (2020 W). For the hot-wire samples, the average hot-wire current was lower for the dynamic wire feeding samples.

Table 5 – Average arc currents, voltages, power and hot-wire current.

Experiment	Arc Current (A)	Arc Voltage (V)	Arc Power (W)	Heat input (J/mm)	HW Current (A)
CW - CWF	171 ± 1	11.7 ± 0.1	2006 ± 14	754	---
CW – DWF	172 ± 1	11.6 ± 0.1	1995 ± 25	750	---
HW – CWF	172 ± 1	11.1 ± 0.1	1922 ± 14	723	73 ± 2
HW - DWF	171 ± 1	11.8 ± 0.1	2020 ± 23	759	71 ± 12

Regarding weld bead geometry, Table 6 shows measured values for each sample and Figure 3 the weld bead cross section macrography's. Experiments with dynamic wire feeding produced weld beads with increased reinforcement, reduced penetration, and narrower width for both cold-wire and hot-wire conditions. The wire's recoil movement during the metal bridge period pulls up the molten pool, while conventional wire feeding pushes the molten pool, leading to wider and lower weld beads.

Figure 3 - Weld beads cross sections. Line in red represents the geometry limits of the CW-CWF sample.

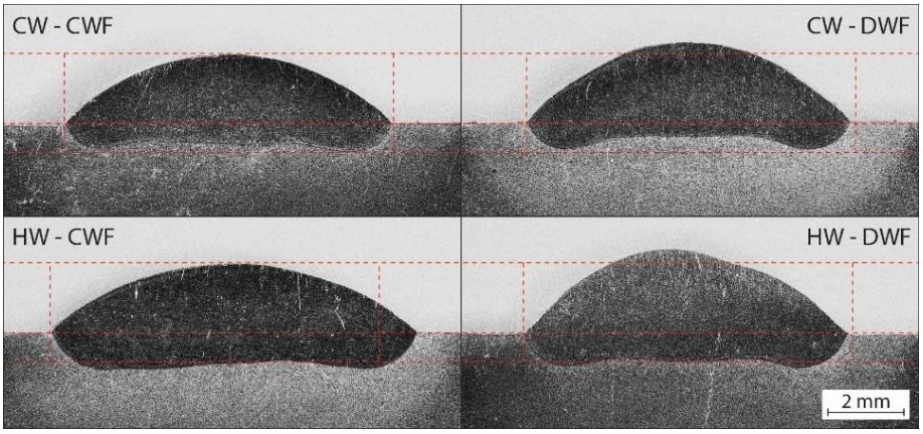

Source: developed by the authors

Comparing cold-wire and hot-wire, the second show weld beads with greater width and penetration, being the HW-CWF sample the wider and deeper weld bead. In this configuration (hot-wire with conventional wire feeding), the pre-heated wire reduces energy needed for melting filler

metal, since part of the energy is absorbed from the molten pool (Chen, Zhang, Huang, Zhang, and Han, 2016). The higher molten pool temperature led to greater penetration. Also, as for the cold-wire, the constant wire feeding also contributes to spread the liquid metal to aside.

Table 6 - Weld beads' geometric profile and dilution

Experiment	Reinforcement (mm)	Width (mm)	Max. Penetration (mm)	Geometric Dilution (%)
CW - CWF	2.04 ± 0.03	9.43 ± 0.18	0.90 ± 0.10	28.2 ± 2.6
CW – DWF	2.29 ± 0.04	9.28 ± 0.38	0.82 ± 0.08	24.4 ± 2.7
HW – CWF	2.01 ± 0.03	10.55 ± 0.22	1.12 ± 0.06	38.4 ± 1.8
HW - DWF	2.46 ± 0.09	9.32 ± 0.99	1.02 ± 0.05	30.1 ± 2.7

Regarding weld bead dilution, the geometrical analysis of the single bead samples showed lower dilution for cold-wire experiments. For the sample carried out with dynamic wire feeding, the dilution was 24.4% and for conventional wire feeding it was 28.2 %, while for hot-wire samples it was 38.4 % and 30.1 % for conventional e dynamic wire feeding, respectively.

For cladded samples, the geometric and chemical dilution had the same behavior as for the single beads (Table 7 – Surface Fe content and dilution of clad samples.. The Fe content measured by optical spectrometry resulted in 11.2 % and 10.9 % for CW-CWF and CW-DWF samples, respectively. For hot-wire experiments, the Fe content was higher, resulting 22.4 % and 19.12 % for conventional and dynamic wire feeding, respectively. These values were considered for chemical dilution analysis, which led to 6.3 % and 6.1 % for cold-wire samples and, 17.8 % and 14.4 % for hot-wire samples, respectively.

Figure 4 - Clad samples cross sections.

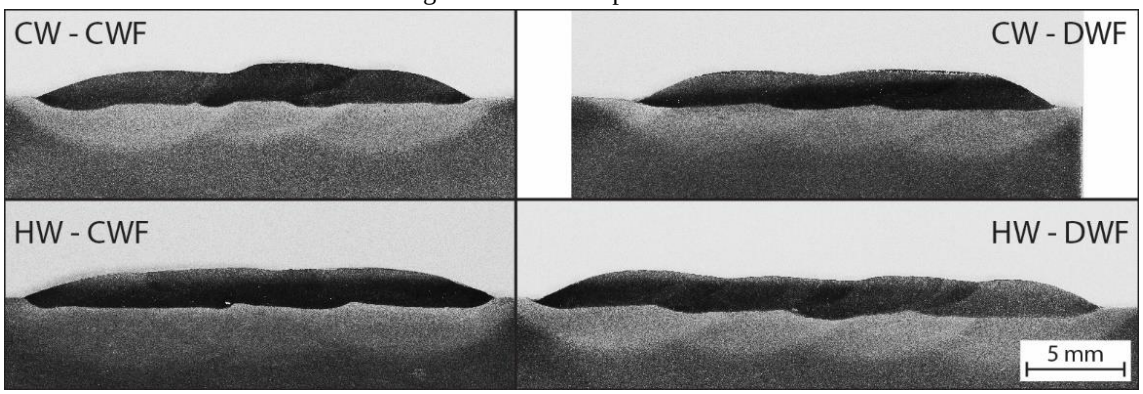

Source: developed by the authors

Table 7 – Surface Fe content and dilution of clad samples.

Overlay	Surface Fe Content (%)	Chemical Dilution (%)	Geometric Dilution (%)

CW - CWF	11.2	6.3	19.0
CW – DWF	10.9	6.1	15.6
HW – CWF	22.4	17.8	24.9
HW - DWF	19.1	14.4	19.8

The greater dilution for hot-wire samples was expected since the wire feeding speed was equal for all samples. Although the temperature of the molten pool was not measured, under similar conditions of arc energy and wire feeding speed in cold-wire configurations, it can be inferred that hot-wire setups result in a hotter molten pool due to less energy being absorbed from the wire.

4. Conclusions

The present study evaluated the GTAW with cold-wire and hot-wire configurations, alongside dynamic wire feeding technique of Inconel 625 single beads and cladded samples. Based on the results obtained, the following conclusions can be drawn:

1- The metal transfer in the dynamic wire feeding is more uniform and stable for the cold-wire than hot-wire configuration. The pre-heated wire leads to a shorter metal bridge period and also the formation of droplets in the wire's tip, which are rapidly transferred to the molten pool by surface tension;

2- For the conditions studied, the arc energy was very close to all experiments since all parameters were kept constat, in exception to the hot-wire current. Even though, the pre-heated wire needs less heat from molten pool to melt, which directly inflect on its temperature (higher temperatures) and on the weld bead geometry. The hot-wire samples resulted in deeper and wider samples.

3- The wire's recoil movement still in metal bridge pulls the liquid metal up by surface tension, which directly influences on the weld bead reinforcement. The samples carried out with dynamic wire feeding resulted in greater reinforcements for both conditions;

4- The hot-wire also led to weld beds with greater dilutions. The Fe content on the cladded surfaces showed better results for the cold-wire samples. Even though, the results obtained showed that higher welding speeds or greater wire feeding speed could be achieved in hot-wire configuration to get lower dilution levels.

5. Acknowledgements

The research presented in this paper is being conducted within the LABSOLDA — Welding and Mechatronics Institute, from Federal University of Santa Catarina, Brazil. The authors are grateful to PETROBRAS and to the Brazilian government agencies CNPq and CAPES for promoting and funding this work.

Referências

A Review on Different Cladding Techniques Employed to Resist Corrosion. (2016).*2016*, *86*(1–2), 51–63. https://doi.org/10.22485/jaei/2016/v86/i1-2/119847

Concurrent Inconel 625 wire and WC powder laser cladding: process stability and microstructural characterisation. (2013). *2013*, *29*(9), 647–653. https://doi.org/10.1179/1743294412Y.0000000073

Contributions of the High Frequency Dynamic Wire Feeding in the GTAW Process for Increased Robustness. (2019). *2019*, *24*(2430), 1–10. https://doi.org/10.1590/0104-9224/SI24.30

Droplet transfer in arcing-wire GTAW. (2016).*2016*, *23*(.), 149–156. https://doi.org/10.1016/j.jmapro.2016.05.014

Effect of vibration and hot-wire gas tungsten arc (GTA) on the geometric shape. (2018).*2018*, *251*(.), 138–145. https://doi.org/10.1016/j.jmatprotec.2017.08.010

Effect of dynamic wire in the GTAW process: Microstructure and corrosion resistance. (2024).*2020*, *285*(.), . https://doi.org/10.1016/j.jmatprotec.2020.116758

Hot-wire GTAW cladding: inconel 625 on 347 stainless steel. (2019).*2019*, *102*(9–12), 3839–3848. https://doi.org/10.1007/s00170-019-03448-0

Influence of weld overlaying methods on microstructure and chemical composition of Inconel 625 boiler pipe coatings. (2014). *2014*, *52*(3), 141–147. https://doi.org/10.4149/km20143141